

INTERIM REPORT

Simulating action potentials in cardiac cells in order to determine the link between atrial fibrillation and ectopic foci in the pulmonary vein

Girish Gupta
School of Physics and Astronomy
University of Manchester

Supervised by Henggui Zhang and Oleg Aslanidi.
Carried out in collaboration with Lucy Foster.

September 2009 – January 2010

Models were made of cardiac cells and their action potentials. These then formed the basis for two- and then three-dimensional models incorporating a cylindrical pulmonary vein. The focus of the work was to determine the link between atrial fibrillation and ectopic foci in the pulmonary vein using computer modelling techniques described in this interim report. The models were stimulated from various points and the geometry modified to more closely resemble actual anatomy. The work is in progress.

Contents

Introduction.....	2
Anatomy and Physiology of the Heart.....	2
The Cell Membrane.....	4
Action Potentials.....	7
Atrial Fibrillation.....	10
Methods and Results.....	11
Single Cell.....	11
Two-Dimensional Cardiac Tissue.....	14
Extension to Two-Dimensional Model.....	14
Three-Dimensional Model.....	16
Discussion.....	19
Conclusion.....	19
References.....	20

Introduction

A computer model of the heart would aid clinicians hugely. Rather than resorting to invasive surgery which would cause the patient much trauma and unnecessary risk, a model would allow clinicians to test their ideas (to a limit of course) with no physical harm caused. As well as surgical techniques, the modelled heart would be allowed to become addled with drugs so clinicians could test the heart's and body's response to them, again with no danger to the patient.

On a prophylactic level, computer models allow scientists to determine the causes of disease in order to combat them more efficiently. It is this branch of the wider project that this report aims to undertake in determining the link between atrial fibrillation and ectopic foci in and around the pulmonary vein.

Our work began as an extension of work carried out by Aslanidi et. al. (2008ⁱ). Their work concentrated on clarifying and confirming their models of single cardiac cells and their action potentials. Our work attempts to extrapolate this to two-dimensional tissues and then three-dimensional models that show a pulmonary vein entering the left atrium and its cardiac tissue.

Our aim was to create a geometrically-accurate framework with which to model various stimuli across the atria and pulmonary vein in order to discover the link between atrial fibrillation and ectopic foci in and around the pulmonary vein.

Anatomy and Physiology of the Heart

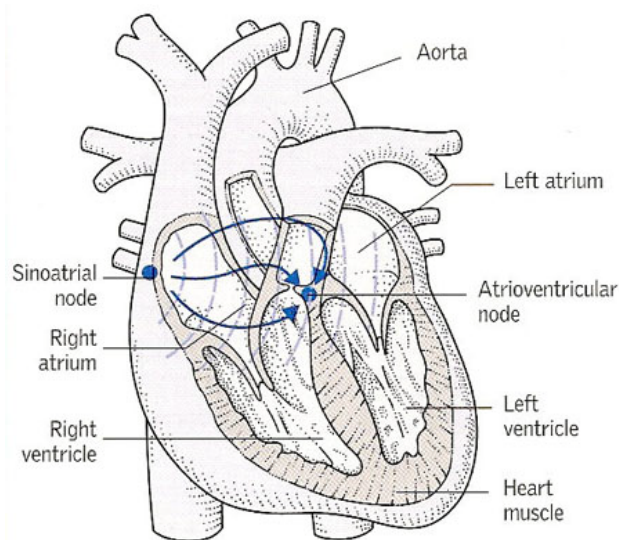


Figure 1 – The human heartⁱⁱ.

The electrophysiology that leads to the heart's pacemaking is primarily initiated at the sinoatrial node, as seen in Figure 1. The sinoatrial node's cells form the 'slow response'

action potential which can be seen as the uppermost action potential in Figure 3. The ‘fast response’ action potentials are detailed below the sinoatrial node’s in Figure 3. The different action potentials will be discussed later.

The electrocardiogram (ECG), while not relevant to this project directly, will aid the explanation of the processes involved in a typical heartbeat. An ECG readout can be found at the bottom of Figure 3. It is essentially a scalar average of the potentials created by the heart’s electrical activity that are found at the body’s surface. Understanding the causes of each part of it allows clinicians to diagnose problems when faced with an atypical ECG.

The sinoatrial node will begin the process with its ‘slow’ action potential. The impulse will pass through the internodal tracts and Bachmann’s bundle (BB, an interatrial tract) to depolarise first the right and then the left atrium. As can be seen by the progression in Figure 3, the atrial muscle then begins to contract. It is this that causes the P wave of the ECG. A lack of P wave indicates a lack of atrial contraction and so is an indicator of atrial fibrillation^[iv, p. 150].

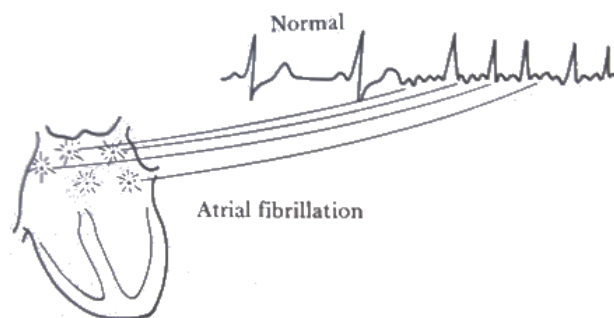


Figure 2 – Atrial fibrillation is indicated on an ECG readout by a lack of P wavesⁱⁱⁱ.

The potential will then arrive at the atrioventricular node before continuing into the bundle of His and onto the Purkinje network to depolarise the ventricular cells. This causes the ventricles to contract to pump blood through the aorta and pulmonary artery to the rest of the body. This is indicated by the QRS complex of the ECG. An extension in the P-Q or P-R interval, therefore, indicates that the potential is taking too long in transit from the atria to ventricles.

The ECG’s T wave is produced by ventricular repolarisation. Atrial repolarisation is masked by the QRS complex^[iv, pp. 141, 146]

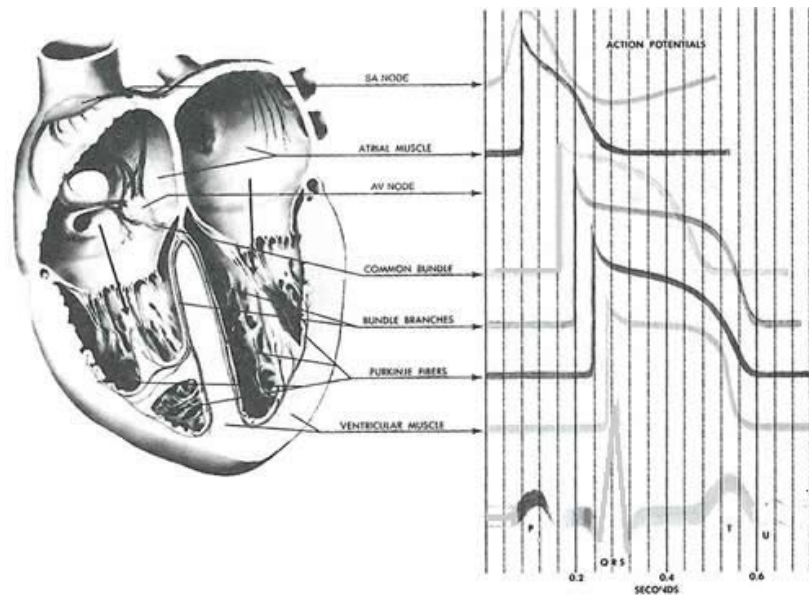


Figure 3 – The human heart and its action potentials, as well as an electrocardiogram readout at the bottom which enables us to ascertain the stage within the heart’s cycle that each action potential is ‘fired’^[iv, p. 143].

It is important to note the different types of cardiac cells for later reference in Figure 10 and Figure 12 especially. Each has a slightly different shape of action potential which shall be described further along.

Cell Type	Acronym
Left atrium	LA
Right atrium	RA
Pulmonary vein	PV
Coronary sinus	CS
Bachmann’s bundle	BB
Cristae terminalis	CT
Pectinate muscle	PM

Table 1 – The different cardiac cell types and their acronyms used throughout this report.

The Cell Membrane

The cell membrane is a phospholipid bilayer that separates the contents of a cell from its exterior. It is across this phospholipid bilayer that action potentials will form due to the variability in permeability of the membrane, to be discussed in *Action Potentials*. This variability is down to electrical and concentration gradients as well as the presence of ion channels and active-transport pumps.

Ion channels are large protein molecules that span the cell membrane. They are specific to ions and allow these through, down their concentration gradient. The channels' permeability to their specific ion is controlled by 'gates'; these open and close when prompted by either the presence of a potential or chemical, i.e., whether their state is open or closed to specific ions will be controlled by either the presence of a potential greater than some threshold or the presence of a chemical stimulus^v.

Sodium-potassium and calcium pumps are also important in the permeability of the membrane. Unlike ion channels which allow an essentially passive processes down a concentration gradient, these pumps actively transport ions against their concentration gradient in order to maintain the resting potential.

For example, in a single procedure, the sodium-potassium pump uses one molecule of adenosine triphosphate (ATP) to pump three sodium ions out of the cell and two potassium ions in^[vi, p. 161].

Despite their huge underlying importance, it is not necessary to go into the specific of the mechanics of the ion channels and pumps. Suffice to say that they play a large role in controlling the permeability of the cell membrane and therefore a large role in the formation and conduction of action potentials through the heart. More in depth work on ion channels formed the basis of the previous work of Aslanidi et. al. that we are extendingⁱ.

Being a means of separating charge, the cell membrane can be modelled as a capacitor circuit, as shown in Figure 4.

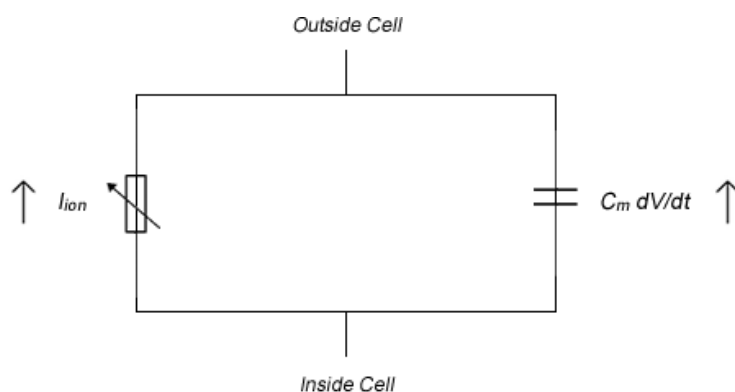


Figure 4 – Electrical circuit model of the cell membrane. Adapted from Keener & Sneyd (1998^[x, p. 57]). The Hodgkin-Huxley model is an extension of this bringing in all ion types.

Assuming this capacitive nature of the cell membrane, it is possible to derive an equation that governs the potential across a membrane in terms of the ions involved and the capacitance (as opposed to the Nernst Equation and its derivative, Equation 2, which deals

with ionic concentration). It is this equation, Equation 1, that is used as the basis for all of our models.

$$C_m \frac{dV}{dt} + I_{ion} = C_m (\nabla \cdot \mathbf{D})(\nabla V)$$

Equation 1 – The membrane potential is governed by this equation. C_m is the membrane capacitance; V is the voltage across it; I_{ion} is the sum of the ions detailed in Table 3; D is the diffusion coefficient^[x, p. 56].

The differing concentrations of various ions inside and outside the cell given in Table 2 cause a potential to exist across the membrane. As described in *Phases of the Action Potential*, the diffusional and electric forces acting on the ions will balance. The potential across the membrane at this steady state is given by Equation 2.

$$E = \frac{RT}{F} \ln \frac{P_K [K]_o + P_{Na} [Na]_o + P_{Cl} [Cl]_i}{P_K [K]_i + P_{Na} [Na]_i + P_{Cl} [Cl]_o}$$

Equation 2 – The equation giving the potential difference across a membrane with concentration $[X]_o$ outside the cell and $[X]_i$ inside the cell. P_x is the permeability of the membrane to the particular ion x . R is the molar gas constant; T is the absolute temperature; F is the Faraday constant.

Equation 2 is an extension of the Nernst equation by Goldman (1943) and later modified by Hodgkin and Katz (1949)^[iv, p. 124]. It gives the potential across a membrane as a function of the permeability of the membrane to particular ions as well as the concentrations of those ions.

Table 2 lists the intra- and extra-cellular concentrations of the most important ions in forming the action potential. It is these figures, when coupled with the permeability of the membrane to them, that are used in Equation 2 to give the resting potential.

Ionic Species	Extracellular concentration (mmol)	Intracellular concentration (mmol)
Na ⁺	145	20
K ⁺	4	150
Cl ⁻	2.5	0.0001

Table 2 – The concentrations of the ionic species both inside and outside the cell. Variations in these concentrations give rise to action potentials^{vii}.

For reference, the ions involved in our models and calculations are detailed in Table 3. As our work is not directly using these for the two- and three-dimensional modelling, they are not mentioned frequently in this report. They are, however, very important in the basis of our work and that of our predecessors.

Total ionic current I_{ion}	
Transient outward potassium current	I_{to}
Long lasting calcium current	I_{CaL}
Transient calcium current	I_{CaT}
Sodium current	I_{Na}
Inward rectifier potassium current	I_{K1}
Delayed rectifier potassium current (rapid)	I_{Kr}
Delayed rectifier potassium current (slow)	I_{Ks}

Table 3 – The different ionic currents modelled. Their potentials are summed to give the action potential^{viii}.

Action Potentials

There are two types of action potential found in the heart: the fast and slow responses^[ix, p. 185]. The slow response occurs solely in the sinoatrial and atrioventricular nodes. These are essentially the pacemakers of the heart, however, the action potentials we shall be concentrating on are the fast responses shown in Figure 5. These exist in the majority of cardiac cells as shown later in Figure 10.

In the early half of the last century, much work was conducted to measure and later quantify the electric signal propagation along giant squid axons (giant for the size of the axon, *not* the squid). Alan Hodgkin and Andrew Huxley developed the first quantitative model of that action potential in 1952, and soon realised its significance in further papers when the word ‘squid’ was excluded from their titles. It was their work that brought about Equation 1^[x, p. 117].
^{xi}. Beeler and Reuter continued the work and applied it to ventricular cells in 1977^[x, p. 149].

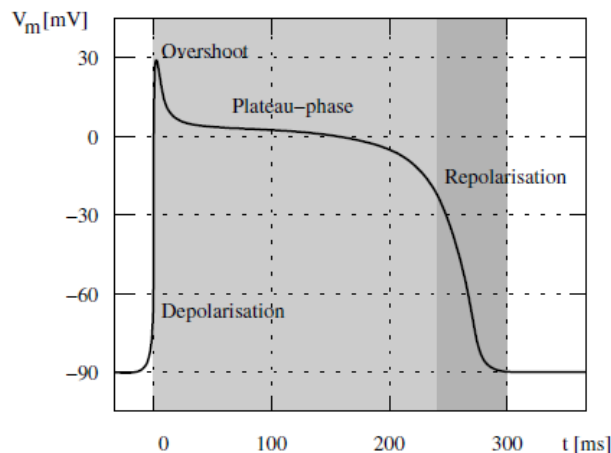


Figure 5 – A typical cardiac action potential with its resting phase at -90 mV, rapid depolarisation, overshoot, plateau phase and repolarisation^[vi, p. 159].

The models demonstrate a typical cardiac action potential, as shown in Figure 5. This shows the potential difference across the membrane of an excitable cell for the period of an action potential. The action potential is caused by ionic currents through the cell membrane, the carriers of which are allowed through by the aforementioned ion channels. The summation of the potentials created by the different ionic currents, shown in Table 3, is the shape shown in Figure 5.

The ions involved are primarily sodium, potassium and calcium. To generate the shape in Figure 5, the membrane permeability varies as a function of time, as do the transmembrane concentration and electrical potential differences.

Following the initiation of the action potential, the cardiac cell will experience a refractory period during which it is unable to initiate another action potential with the ease of the first. This is down to inactivation of the Na⁺ channels. The refractory period is split into an absolute period and a relative one. During the absolute refractory period, an action potential cannot be initiated no matter how high the stimulus. This lasts for a short period before the onset of the relative refractory period during which a much higher stimulus than the usual threshold is required to initiate an action potential^[iv, p. 126].

This refractory period is important in conduction of stimuli. It prevents the electrical impulse going backwards along a pathway as the state (open or closed) of the previous ion channel will not be altered by the potential in and around the current ion channel until the refractory period is over, by which time the stimulus will have moved on.

Phases of the Action Potential^{xii}

The resting potential is governed primarily by potassium and sodium ion concentrations. Two opposing forces lead to an equilibrium voltage difference caused by the differing potassium ion concentrations. One is the chemical force, based on the concentration gradient; this leads to an outward current (where current is conventionally positive and so this implies an outward K⁺ flow, for example). The other is the electrostatic force which leads to an inward current as there is a significant concentration of negative ions left residing within the cell; this leads to an inward current.

On inserting the measured values of these concentrations in Equation 2 and taking into account the other ions flowing through the membrane, the value for the resting potential is roughly -90mV.

The following should be read with reference to Figure 5.

On the application of a stimulus to a threshold level of roughly -65mV , an action potential is produced. This is begun with a rapid depolarisation of the potential. This is due almost solely to an influx of sodium ions through the cell membrane; this is the I_{Na} of Table 3. Many of the drugs used to treat some types of cardiac arrhythmias work by blocking the ‘fast’ Na^+ channels that allow this depolarisation.

There is a small notch—labelled ‘overshoot’ in Figure 5—showing the beginnings of repolarisation. This is caused by a cessation of I_{Na} and the activation of the transient outward potassium current, I_{to} . Liu et. al. (1993^{xiii}) demonstrated the link between the size of the notch to both the type of cardiac cell in question as well as the basic cycle length (BCL). The greater the BCL, the larger the notch and the further inside the heart the cell, the smaller the notch, i.e., endocardial cells have smaller repolarisation phases. This is demonstrated in Figure 6 and will be used later to confirm the accuracy our own work.

A plateau then occurs. There is a dual effect from the influx of Ca^{2+} and the efflux of K^+ , described by I_{CaL} and I_{Ks} respectively. When the efflux of potassium exceeds the influx of calcium, the cell finally begins to repolarise back to its resting potential. The transient outward potassium current (I_{to}) and delayed rectifier potassium (I_{Kr} and I_{Ks}) currents help initiate this phase.

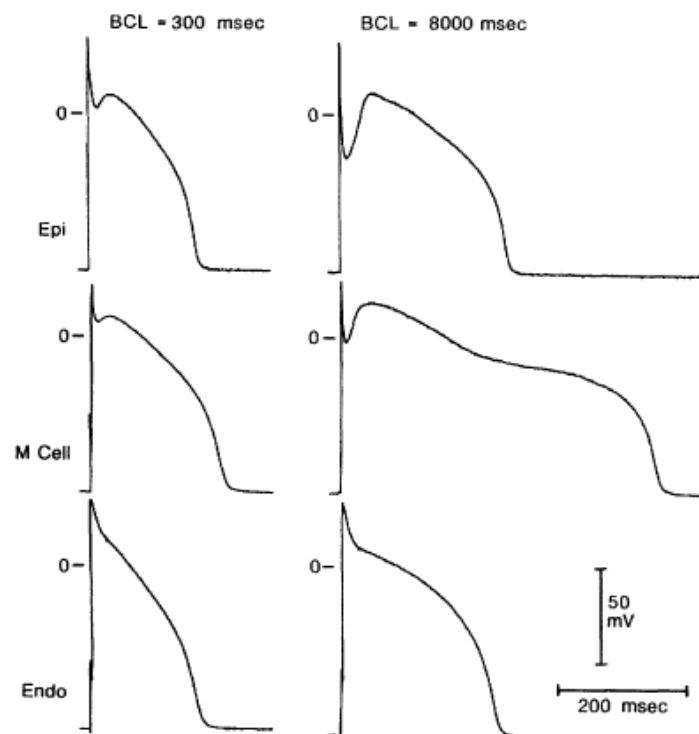


Figure 6 – Liu et. al. (1993^{xiii}) showed experimentally that as BCL increased, the size of the notch showing the beginnings of repolarisation (left vs. right of figure). They also showed that the notch decreased in size as action potentials ‘progressed’ into the heart, i.e., epicardial cells have a larger notch than endocardial cells (bottom to top of figure). (M stands for midmyocardial.)

Atrial Fibrillation

Atrial fibrillation is the most common form of cardiac arrhythmia, though is poorly understood^{xiv,xv,xvi}. Chard and Tabrizchi (2009^{xiv}) wrote of the link between the pulmonary vein and atrial fibrillation physiology following the discovery of the phenomenon by Haissaguerre et. al. just over a decade earlier^{xvi}.

Haissaguerre et. al. studied 45 patients with atrial fibrillation and found that 94 per cent of ectopic foci were located in the pulmonary vein (varying between the left and right superior and inferior). Their conclusion was that the pulmonary vein is “an important source of ectopic beats [which would lead to] atrial fibrillation”^{xvi}. The results are shown graphically in Figure 7.

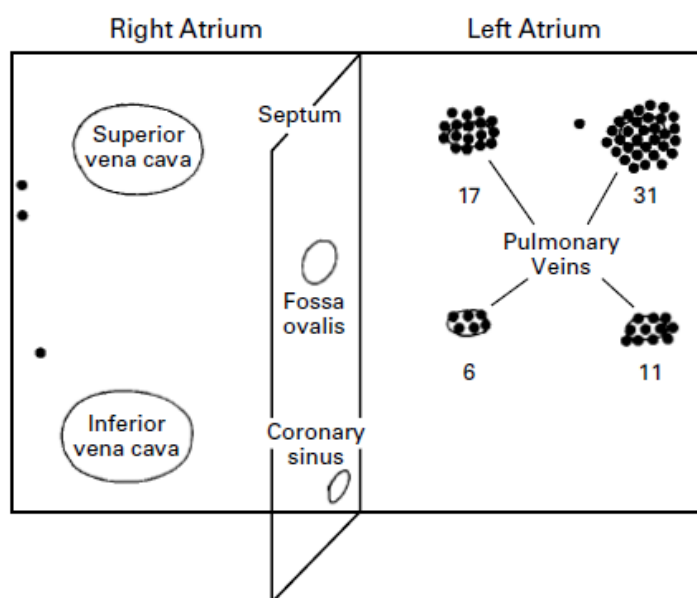


Figure 7 – “Diagram of the sites of 69 foci triggering atrial fibrillation in 45 patients. Note the clustering in the pulmonary veins, particularly in both superior pulmonary veins. Numbers indicate the distribution of foci in the pulmonary veins.”—Haissaguerre et. al., 1998^{xvi}.

Their idea was that pacemaking cells within the pulmonary vein can produce electrical signals which interfere with those propagating from the sinoatrial node. This interference leads to so-called ‘re-entry’.

Re-entry is a re-excitation of an area through which an electrical impulse has already passed. There are two types of re-entrant circuits described by Berne and Levy (2000^{ix}, pp. 195-196): When the circuit is fixed in one region of the heart, the loop can lead to tachycardia—raised heartbeat. When the loop, however, consists of “multiple, highly irregular continuously moving re-entrant circuits,” this can lead to atrial (or ventricular) fibrillation.

Spiral waves form within the area experiencing fibrillation. These do not require a repeating source to exist, as they are typically self-sustained. This is a reason that they are generally only found in pathophysiological situations, i.e., abnormal and unhealthy situations^[x, p. 305].

Atrial fibrillation can be present in a patient for many years with no serious side-effects barring an occasional shortness of breath. However, due to its irregular nature, patients are susceptible to the formation of blood clots in or around the re-entry loops. If these clots make their way through the carotid artery up to the brain, this could lead to stroke, a rapid loss of brain function due to a lack of blood to the brain which could cause permanent neurological damage and death. Ventricular fibrillation, incidentally, cannot be left for a sustained period without treatment as its presence will lead to a cessation of blood pumping around the body. Defibrillation would then be immediately essential.

Methods and Results

Single Cell

The first experiment worked on single cells and their action potentials. This was essentially a re-run and confirmation of the work of Aslanidi et. al. (2008ⁱ). It used Equation 1 as a basis for producing the action potentials of various cell types (Figure 10) and a restitution curve (Figure 8) which demonstrates the trend of the APD at various BCLs.

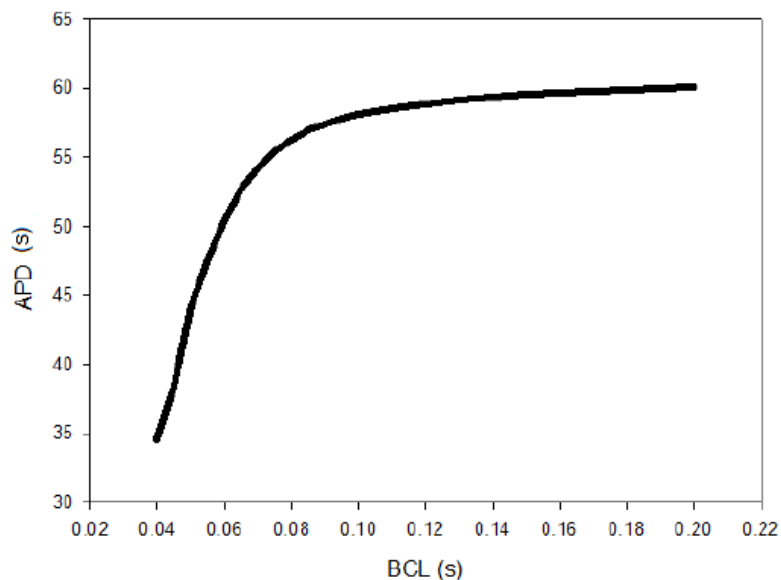


Figure 8 – Restitution Curve

Figure 10 shows the action potentials produced by various cardiac cell types. They all differ slightly in their shape but follow the same general trend. The particulars of the shape were

discussed earlier in *Phases of the Action Potential*. Our work agrees with the experimental data of Liu et. al. (1993^{xiii}).

Figure 8 shows a restitution curve. This is a graph showing the action potential duration as a function of the BCL. It shows that a low BCL will allow for a shorter APD, while increasing BCL, up to a point will shorten the lengthen the APD.

Figure 9 shows the difference in action potential as a function of BCL. It correlates with the work of Liu et. al. in 1993 demonstrated in Figure 6 and spoken about in *Phases of the Action Potential* earlier.

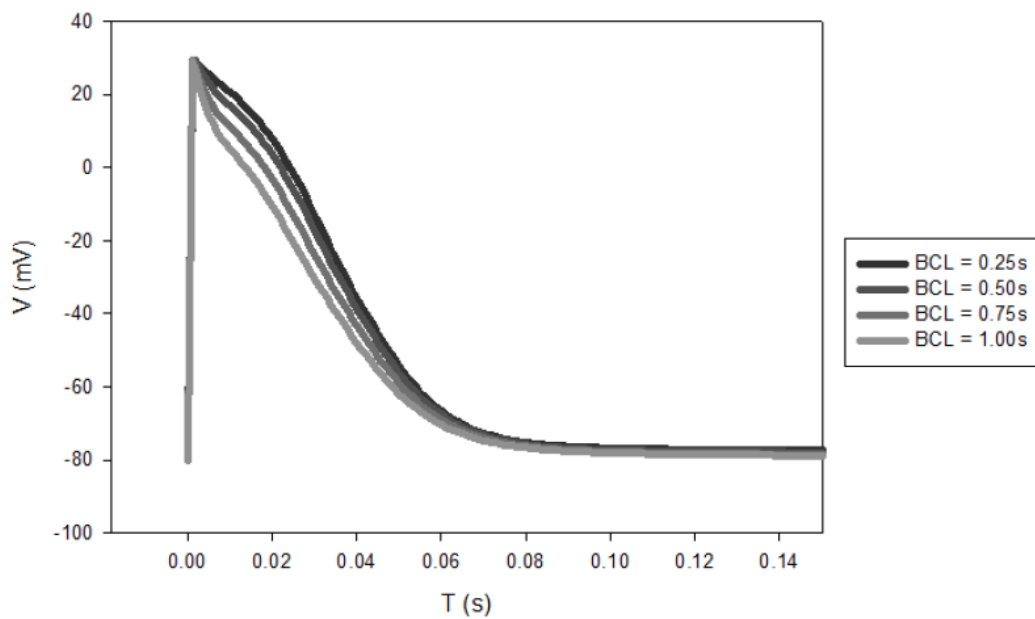


Figure 9 - Action potentials at varying basic cycle lengths (BCLs).

This work shows that the basis for our further models, the two- and three-dimensional work, is correct, following and correlating with previously published experimental work. Confirmation of this allowed us to continue to two- and three-dimensional models.

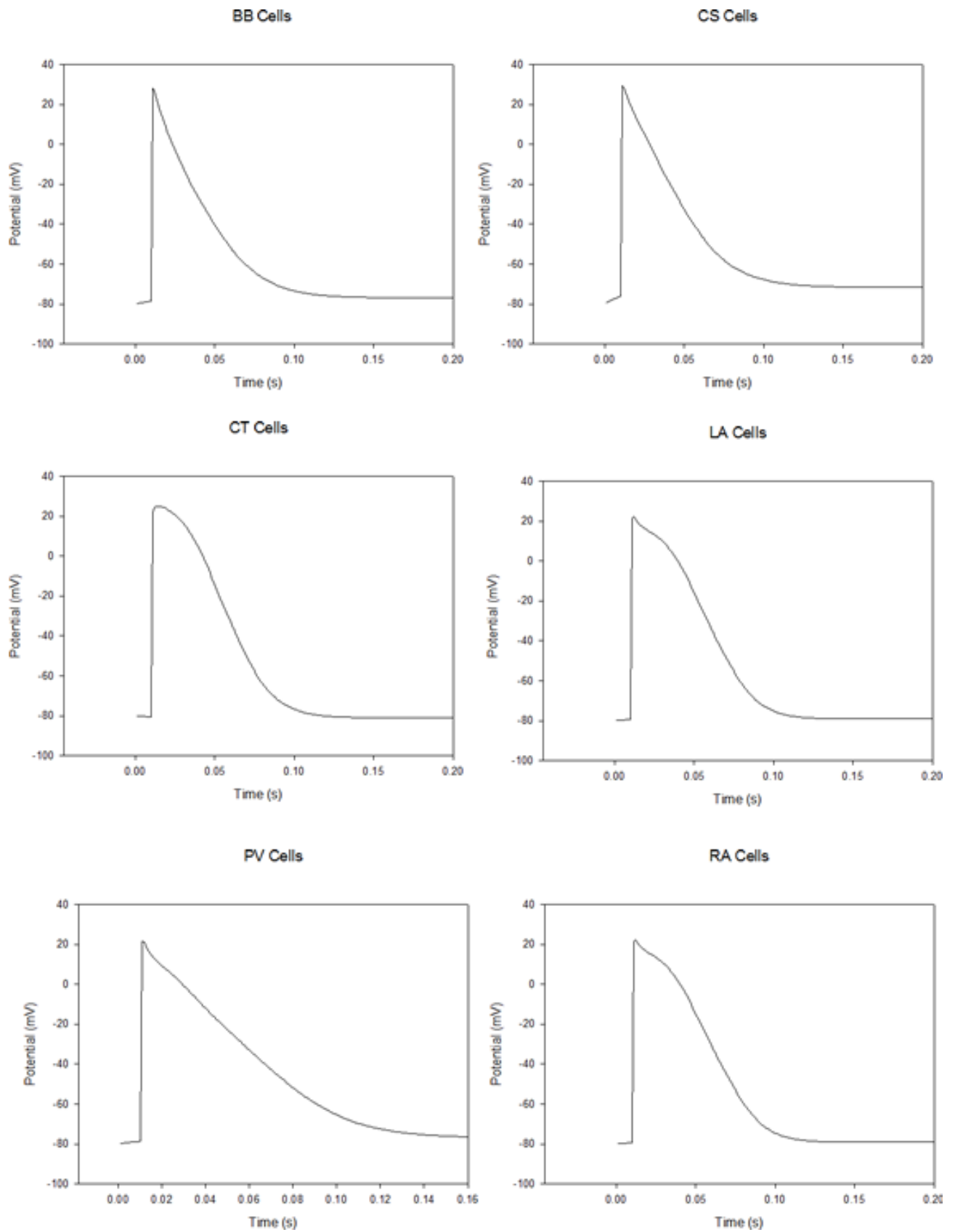


Figure 10 – Action potentials of different cardiac cells, c.f., Figure 3 and Figure 5. Refer to Table 1 for explanation of acronyms.

Two-Dimensional Cardiac Tissue

Our two-dimensional model, again, was based on the same previous workⁱ. However, many modifications were made in order to correct it and tailor it to our requirements that concentrate on the pulmonary vein.

Figure 11 shows the visual output of the model. It is split into three distinct layers. The middle section of the image should be seen as the right atrium, the lowest section as the left atrium while the uppermost strip signifies a flat sheet that is curled into a cylinder representing the pulmonary vein; this will be described in the following section.

The red colour of Figure 11 (and Figure 13 and Figure 14) indicates a raised voltage (darker red implies higher voltage) while the blue indicates cells not currently at a raised potential.

Its exact geometry, i.e., locations of each cell type, is demonstrated by the flat section of Figure 12 ignoring the pulmonary vein.

This two-dimensional model and the following extension to it, shown in Figure 11, were repeated a large number of times with varying parameters such as the diffusion coefficient and the diameter of the pulmonary vein.

Extension to Two-Dimensional Model

An attempt was made to extend this two-dimensional model to three dimensions by adding a rectangle of pulmonary vein cells to it, whose boundary conditions would force it to roll into a cylinder and connect to the circumference of the 'hole' in the left atrium of Figure 11. This is, of course, abstract in that it would not be visualised as a three-dimensional model, however, it would demonstrate the same characteristics.

Spiral waves can be seen forming in the atria, however, their excitation is not extending into the pulmonary vein, the uppermost strip. Neither is there yet any evidence of self-oscillation in the pulmonary vein. Due to the abstract nature of this model, we thought it preferable to look into a different way of constructing a three-dimensional model.

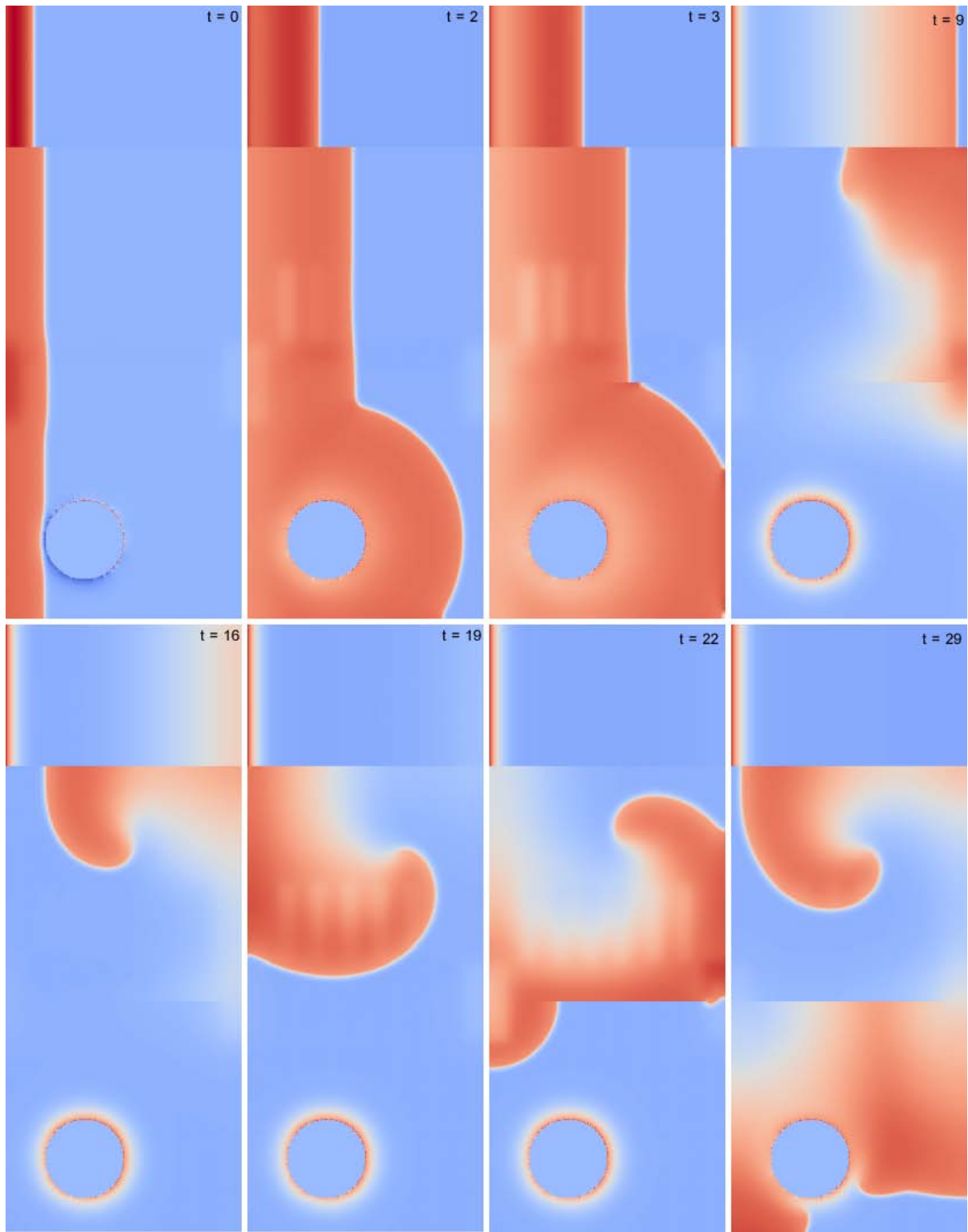


Figure 11 – This two-dimensional model contains three distinct strips from top to bottom. The second represents the right atrium, the lower the left atrium with the pulmonary vein ‘hole’ clearly marked and the upper depicts the surface which is curved, by boundary conditions, into a cylinder and connected to the edge of the pulmonary vein hole. The system is stimulated from the base of the atria as well as the base of the pulmonary vein. Spiral waves are seen forming in both atria. The t signifies equal time steps.

Three-Dimensional Model

The three dimensional model required a matrix, created by our code, which indicated the cell type in a particular region. This geometry can be seen in Figure 12. It shows the locations of the difference types of cell indicated by the action potentials of Figure 10. This geometry allowed for the cells in the cardiac tissue as in our two-dimensional model to be arranged as a surface out of which the pulmonary vein emanated.

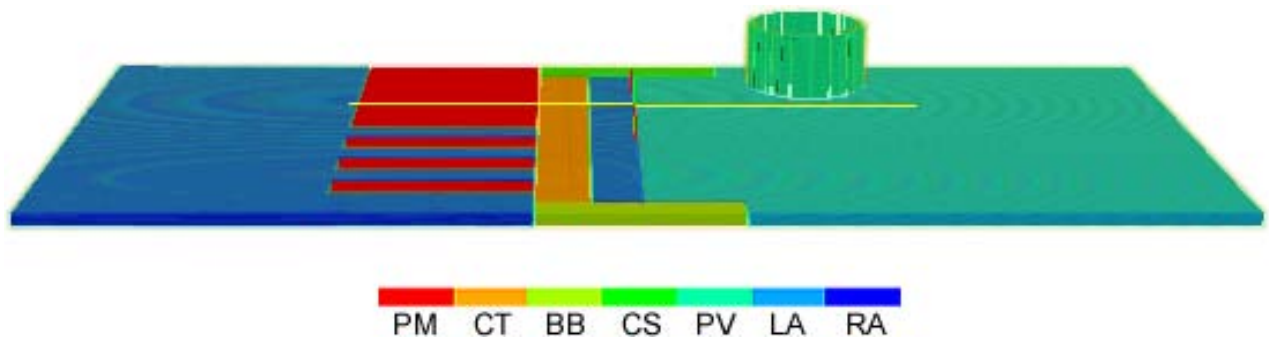


Figure 12 – The geometry of our three-dimensional model. The key shows the cell type indicated by the associated colour; refer to Table 1 for explanation of the acronyms. The cells' action potentials can be seen in Figure 10.

Note: The pulmonary vein appears broken. This is due solely to the effects of scaling the geometry file down to speed up visualisation for creation of this image. The actual visualisations (Figure 13 and Figure 14) of the code do not contain a broken pulmonary vein.

Figure 13 shows the spread of a potential across our model when the stimulus was applied along the bottom (of the figure, i.e., the base of the left and right atria). This of course does not demonstrate our aim of finding a link between pulmonary vein ectopic foci and atrial fibrillation.

Figure 14 works towards that goal by stimulating both the base of the atria, as in Figure 13, but also the top of the pulmonary vein. The excitation can be seen travelling down the pulmonary vein and into the left atrium. Spiral waves are seen in both atria. However, there is no further excitation or self-oscillation in the pulmonary vein.

Work shall be done in changing the parameters of this model, similarly to the two-dimensional model, in pulmonary vein diameter and the general anatomy. This shall be discussed further in the *Discussion*.

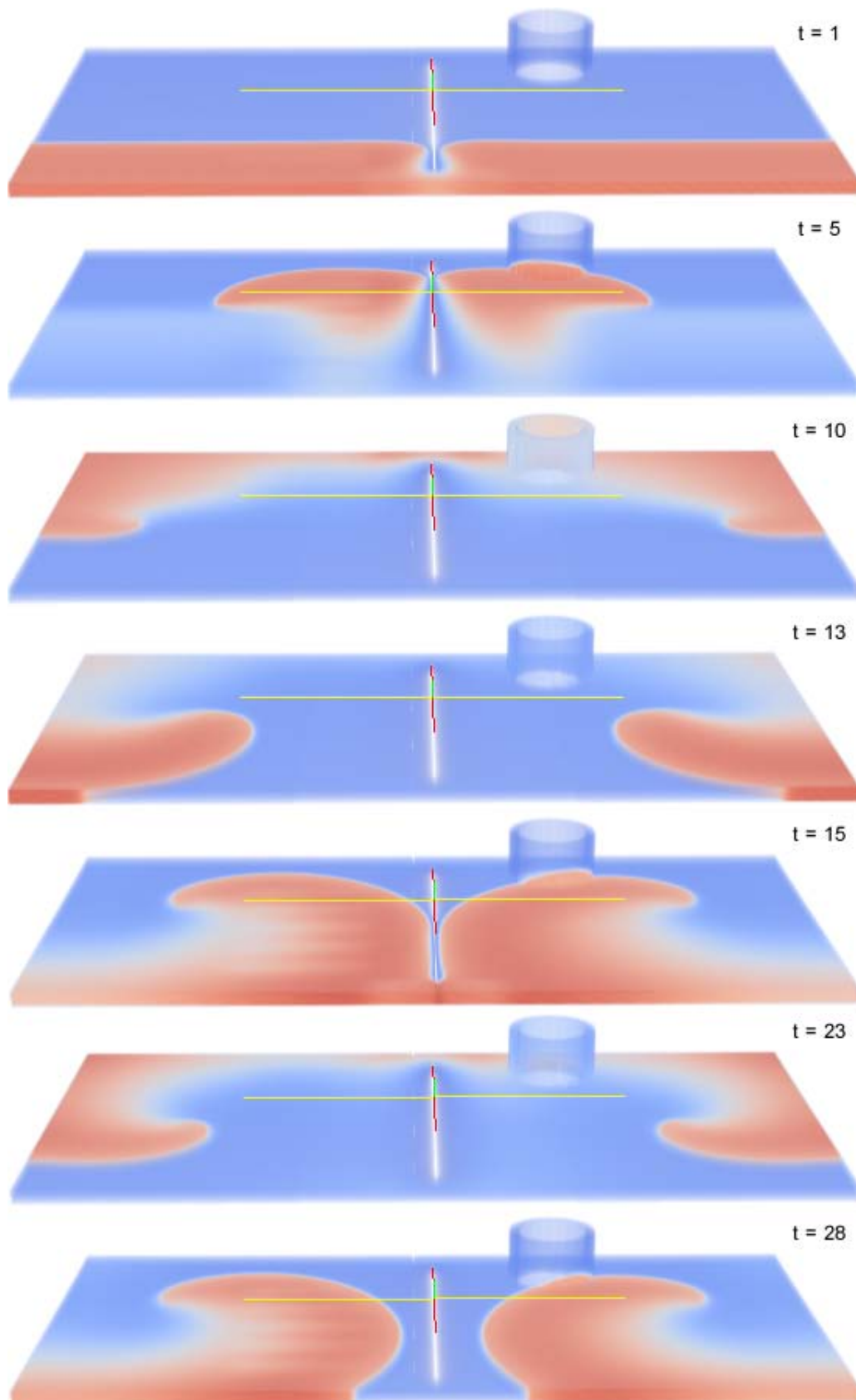


Figure 13 – Our first three-dimensional model—to be viewed with reference to Figure 12 for its geometry—is stimulated solely from the base of the atria. Spiral waves are seen forming in both atria and covering the cylindrical pulmonary vein. The t signifies equal time steps.

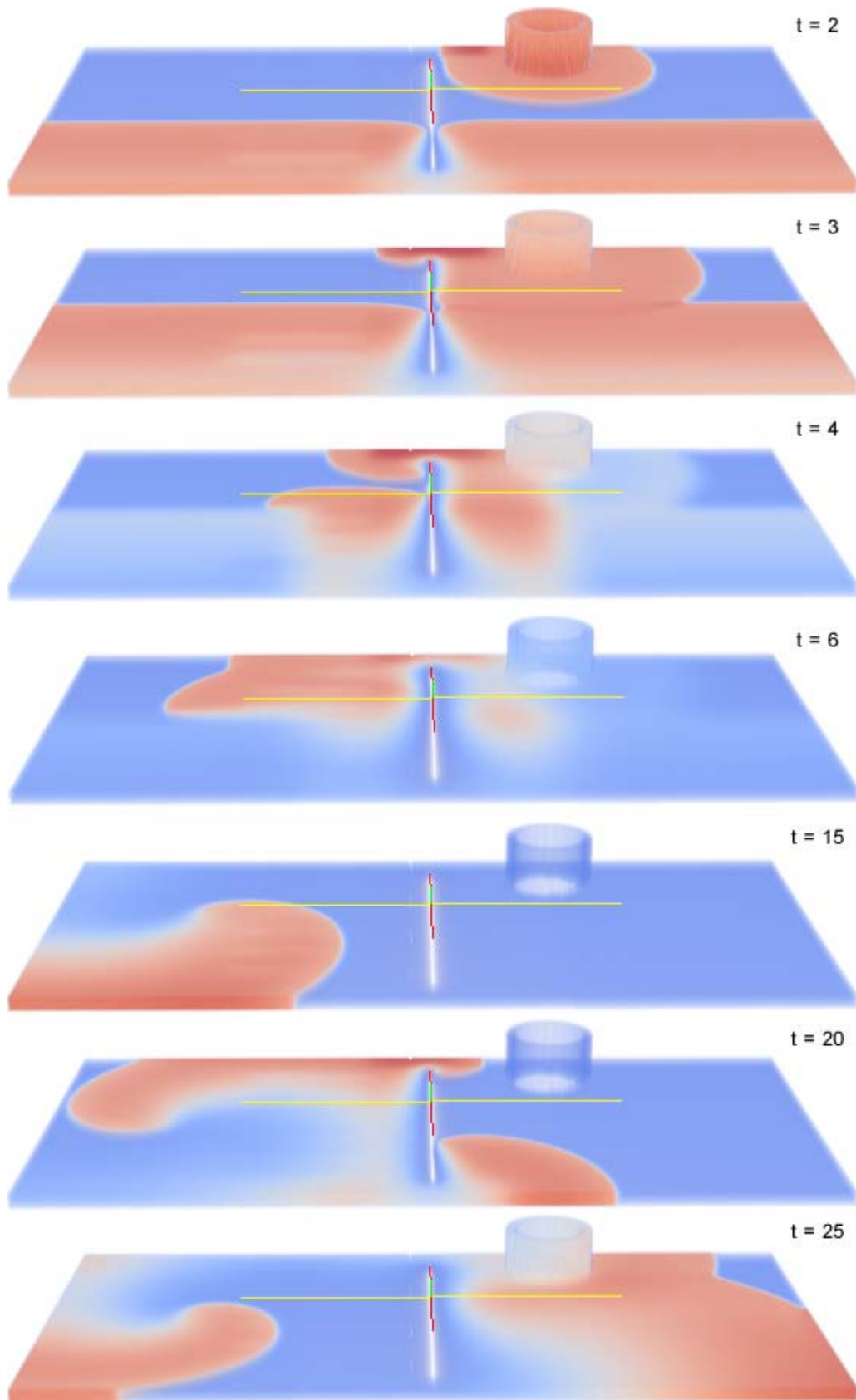


Figure 14 – Based on the same geometry as Figure 13, this model is stimulated as Figure 13 at the base of the atria but also at the top of the pulmonary vein. Again spiral waves form, however, do not self-oscillate within the pulmonary vein. The t signifies equal time steps.

Discussion

The work completed so far has demonstrated that our aim of determining the link between ectopic foci in the pulmonary vein and atrial fibrillation can be achieved.

This three-dimensional matrix model is easily understood, very simply visualised and requires no complex boundary conditions. We have the excitation wave travelling across its cells as expected and are able to view this, and so counter problems, with ease.

Our next task is to stimulate our three-dimensional model—that shown in Figure 13—at the pulmonary vein as well as at the base of the atria. This will bring us closer to discovering a link between ectopic foci at the pulmonary vein and atrial fibrillation.

We will also modify the matrix that describes the geometry of the cardiac cells to make it more closely resemble that of the heart. It is all well and good having a working model showing that atrial fibrillation occurs with a perfectly cylindrical pulmonary vein touching cardiac tissue at its edges, however, this is unrealistic. A computer model is worthless unless it resembles reality.

There are many papers covering the anatomy of the heart which we shall use to perfect our geometry. Nathan and Eliakim (1966^{xvii}) went into much detail of human cardiac anatomy.

Once this has been completed, our model should demonstrate our aim successfully.

Another aim is to study the conditions required for self-oscillations. This was mentioned briefly in both the two- and three-dimensional models. It could be that an ectopic focus emerges in the pulmonary vein without direct stimulation; this would then interact with any atrial fibrillation.

Conclusion

we have begun the process of creating a computational method for studying the link between atrial fibrillation and ectopic foci in the pulmonary vein.

Beginning with a single cell model, we have extended this to two-dimensional tissue—with an attempt at adding a quasi-three-dimensional pulmonary vein—to a complete three-dimensional model which we will make further geometrically accurate.

Stimulations have been set from the base of the atria and at the top of the pulmonary vein. These, much like the geometry, will be refined to reflect more closely a realistic situation.

Our work so far is a strong basis to continue and achieve our aim in forthcoming work.

References

- ⁱ Aslanidi, O.V., Dewey, R.S., Morgan, A.R., Boyett, M.R., Zhang, H. 2008, 'Regional differences in rabbit atrial action potential properties: mechanisms, consequences and pharmacological implications', *Conf. Proc. IEEE Eng. Med. Biol. Soc.*, pp. 141-144.
- ⁱⁱ Darling, D. <http://www.daviddarling.info/encyclopedia/S/sinoatrial_node.html>. (Image used with permission.)
- ⁱⁱⁱ Phibbs, B. 1975, *The Human Heart*, Mosby, St Louis.
- ^{iv} Webster, J.G. 1998, *Medical Instrumentation*, John Wiley & Sons, New York.
- ^v Seeley, R.R., Stephens, T.D., Tate 1995, *Anatomy & Physiology*, Mosby, St Louis, p. 267.
- ^{vi} Sachse, F. 2004, *Cardiac Electrophysiology*, Springer, Berlin, p. 159.
- ^{vii} Klabunde, R.E. <<http://www.cvphysiology.com/Arrhythmias/A007.htm>>.
- ^{viii} Lindblad, D.S., Murphey, C.R., Clark, W., Giles, W.R. 1966, 'A model of the action potential and underlying membrane currents in a rabbit atrial cell', *Sp. Comm. Am. Physiol. Soc.*, pp. 1666-1696.
- ^{ix} Berne, R.M., Levy, M.N. 2000, *Principles of Physiology*, Modsbay, Missouri, pp. 195-196.
- ^x Keener, J., Sneyd, J. 1998, *Mathematical Physiology*, Springer, New York.
- ^{xi} Hodgkin, A., Huxley, A 1952, 'A quantitative description of membrane current and its application to conduction and excitation in nerve', *J. Physiol.*, no. 117, pp. 500-544.
- ^{xii} Berne, R.M., Levy, M.N. 1998, *Physiology*, Mosby, Missouri, pp. 330-338.
- ^{xiii} Liu, D.W., Gintant, G.A., Antzelevitch, C. 1993, 'Ionic bases for electrophysiological distinctions among epicardial, midmyocardial, and myocytes from the free wall of the canine left ventricle', *Circ. Res.*, vol. 72, pp. 671-687.
- ^{xiv} Chard, M., Tabrizchi, R. 2009, 'The role of pulmonary veins in atrial fibrillation: A complex yet simple story', *Pharm. & Ther.*, no. 124, pp. 207-218.
- ^{xv} Atienza, F., Jalife, J. 2007, 'Reentry and atrial fibrillation', *Heart Rhythm. Soc.*
- ^{xvi} Haissaguerre, M et. al. 1998, 'Spontaneous initiation of atrial fibrillation by ectopic beats originating in the pulmonary veins', *New England Journ. of Med.*, vol. 339, no. 10, pp. 659-666.
- ^{xvii} Nathan, H., Eliakim, M. 1966, 'The junction between the left atrium and the pulmonary veins: an anatomic study of human hearts', *Circulation*, vol. 34, pp. 412-422.